Eur. Phys. J. B **41**, 171–175 (2004)
DOI: 10.1140/epjb/e2004-00306-7

THE EUROPEAN PHYSICAL JOURNAL B

Surface effects in α-Fe_2O_3 nanoparticles

R.D. Zysler[1,a,b], M. Vasquez Mansilla[1], and D. Fiorani[2]

[1] Centro Atómico Bariloche, 8400 S.C. de Bariloche, RN, Argentina
[2] ISM-CNR, Area della Ricerca di Roma, C.P. 10, 00016 Monterotondo, Roma, Italy

Received 20 February 2004
Published online 12 October 2004 –

Abstract. The magnetic properties of 5 nm α-Fe_2O_3 nanoparticles have been investigated by magnetization measurements on a sample consisting of homogeneously dispersed, non-interacting, nanoparticles in a polymer matrix. The results indicate that the magnetic properties are mainly determined by surface effects, which manifest themselves in high coercive field, high irreversibility field and shifted hysteresis loop, after field cooling. These effects come from surface anisotropy and exchange anisotropy, due to the coupling between the disordered surface magnetic structure, with multiple spin configurations, and the core antiferromagnetically ordered structure.

PACS. 75.50.Tt Fine-particle systems; nanocrystalline materials – 75.75.+a Magnetic properties of nanostructures – 75.70.Rf Surface magnetism – 75.50.Ee Antiferromagnetics

Introduction

Surface effects in magnetic particles have been the subject of growing interest in recent years from both an experimental and theoretical point of view [1–7]. They are increasingly important as the particle size decreases, because of the increase in surface to volume ratio. The modification of structural and electronic properties near and at the particle surface results in breaking of lattice symmetry and broken bonds, which give rise to site specific surface anisotropy, weakened exchange coupling and surface spin disorder. Moreover, spin coupling at the interface between different surface and core magnetic structures can give rise to exchange anisotropy. In concentrated nanoparticle systems, interparticle exchange interactions, involving surface atoms, are possible if particles are in close contact. In particular, surface effects play a dominant role on the magnetic behaviour of antiferromagnetic nanoparticles, due to their small intrinsic core magnetic moment. Due to their potential for investigating surface effects and magnetization reversal by quantum tunneling [8], antiferromagnetic nanoparticles have received renewed interest in recent years [9–15].

In this context, α-Fe_2O_3 antiferromagnetic nanoparticles deserve special attention, although hematite is not an archetypal antiferromagnet. Indeed, below the Néel temperature (T_N = 960 K) the bulk material undergoes a first-order magnetic transition at T_M = 263 K (Morin temperature). Below T_M, the spins are antiparallel and oriented along the trigonal [111] axis (c-axis) and the material behaves as a uniaxial antiferromagnet (AF). On the other hand, above T_M spins lie in the basal plane, perpendicular to the [111] axis except for a slight spin canting (∼1 min of arc) out of the plane [16,17], resulting from the Dzialoshinski-Moriya anisotropic exchange interaction, which is responsible for a small net magnetic moment (weak-ferromagnetism). The Morin temperature was found to be strongly dependent on the particle size, decreasing with it and tending to vanish below a diameter of ∼8 nm, for spherical particles [18]. Strains, crystal defects (e.g. low crystallinity of the particles, vacancies), stoichiometric deviations and surface effects also tend to reduce T_M [19].

In this paper, we investigated by means of magnetization measurements the magnetic properties of ∼5 nm α-Fe_2O_3 nanoparticles homogeneously dispersed in a polymer matrix. The results provide clear evidence of surface and exchange anisotropy effects.

Experimental procedure

Dispersed hematite nanoparticles were obtained by hydrolysis of iron etoxide and adding the FeOOH nanoparticles from the hydrolysis process to a PVA solution (PM 72000) and a subsequent aging in boiling water for 10 days. The final hematite concentration was 14% in weight, which is equivalent to 3.6% in volume fraction.

[a] e-mail: zysler@cab.cnea.gov.ar
[b] Member of the Consejo Nacional de Investigaciones Científicas y Técnicas, Argentina.

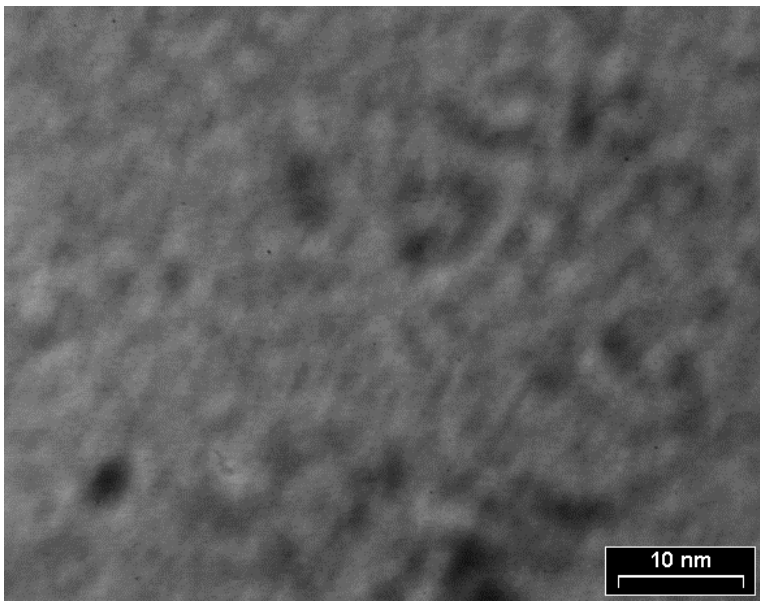

Fig. 1. Bright-field micrograph of hematite particles.

The structural properties were investigated by transmission electron microscopy (TEM) and X-ray diffraction (Philips PW 1710) measurements.

The magnetic properties were investigated in the temperature range 5–300 K by magnetization measurements using a commercial SQUID magnetometer (H_{max} = 55 kOe).

Results

In Figure 1 we show a TEM image of the sample. The mean particle diameter is 5 nm ± 2 nm. In the X-ray diffraction measurement on the sample, only a very broad reflection is observed, essentially due to the polymeric matrix, covering the iron oxide reflections, which are expected to be broad, due to the small particle size and the low crystallinity of the particles. Mössbauer measurements indicate that the particles consist of a hematite core and a less crystalline shell [20].

The magnetization versus temperature measurements were performed from 5 to 300 K, under zero-field cooling (ZFC) and field cooling (FC) conditions, with an applied field H = 50 Oe (Fig. 2). There is no evidence of Morin transition, characterized by a sharp jump of the magnetization with increasing temperature. This is expected, because of the small size of particles. The observed behaviour is typical of an assembly of single-domain magnetic nanoparticles. It is characterized by the existence of two regimes: an equilibrium high temperature regime (superparamagnetic regime), where particle moments are free to thermally fluctuate, and a non-equilibrium low temperature regime (blocked regime), where particle moments are blocked along their anisotropy

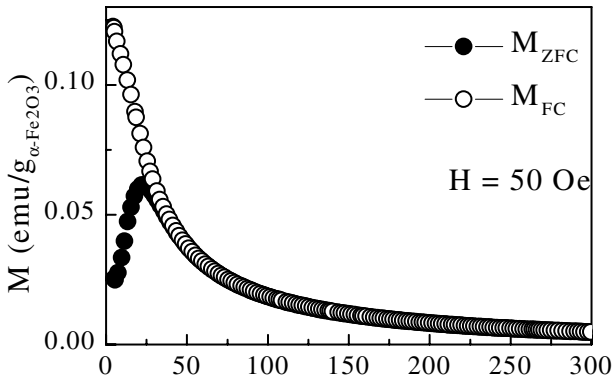

Fig. 2. Temperature dependence of the ZFC (solid circles) and FC (open circles) magnetization measured at 50 Oe.

directions. With decreasing temperature, particle moments block progressively, according to the distribution of their blocking temperatures (T_B). This gives rise to magnetic irreversibility and to a maximum of the low field ZFC magnetization at a temperature T_{max}, which is proportional to the average blocking temperature $\langle T_B \rangle$, the proportionality constant depending on the type of particle size distribution function. The ZFC magnetization shows a maximum at $T_{max} \sim 22$ K. As usually observed in non interacting nanoparticle systems, the M_{FC} curve increases continuously with decreasing temperature, following a Curie-Weiss law even below T_{max} (small deviations are observed below ∼15 K). The ZFC and FC magnetization curves split at $T_{irr} = 40$ K. For an assembly of non-interacting nanoparticles with size distribution, the T_{irr} value corresponds to the highest T_B value, i.e. to that of particles with highest energy barrier; therefore,

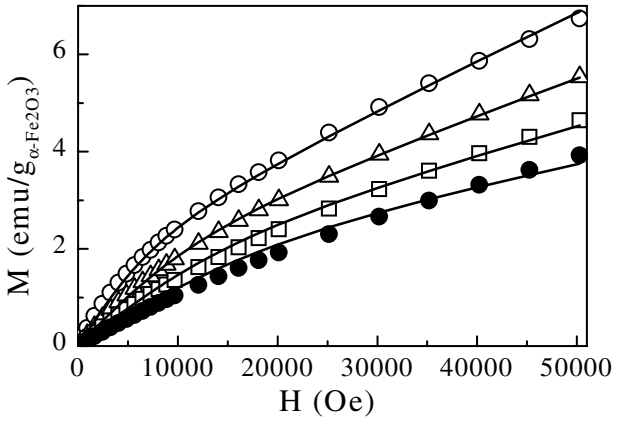

Fig. 3. Magnetization versus applied field at different temperatures for $T > T_{irr}$ (superparamagnetic regime): 100 K (open circles (○)), 150 K (up triangles (△)), 200 K (squares (□)), and 250 K (solid circles (●)). The solid lines result from the fitting of the magnetization (see text).

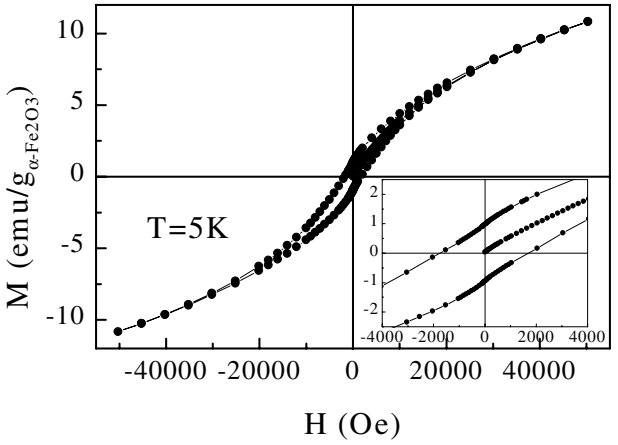

Fig. 4. Magnetization cycle at 5 K. The inset shows the low field magnetization behaviour.

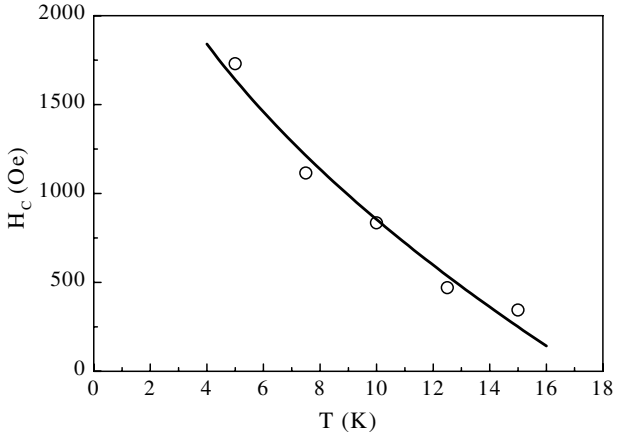

Fig. 5. H_C as a function of temperature. The solid line corresponds to a $T^{1/2}$ law fit with $H_C(T = 0) = 3500(250)$ Oe and $T_B = 17(1)$ K.

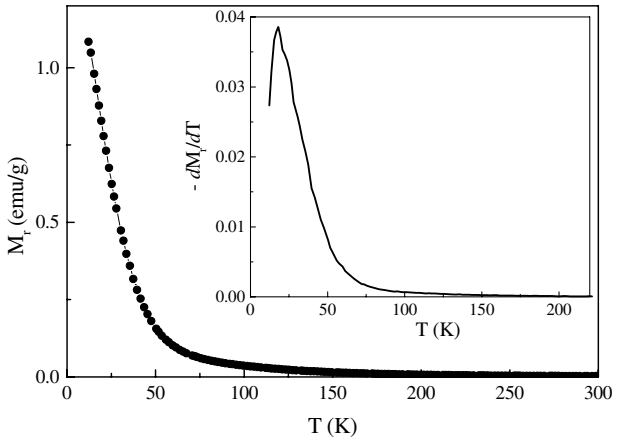

Fig. 6. Remanent magnetization as a function of temperature. Inset: temperature derivative of the remanence curve.

the difference between T_{irr} and T_{max} gives a measure of the energy barrier distribution, mainly determined by the particle size distribution (e.g., for uniaxial particles: $E_B = K_aV$, where K_a is the uniaxial anisotropy constant and V is the particle volume).

Isothermal magnetization measurements were performed at different temperatures in fields up to 50 kOe. In Figure 3, some curves recorded above T_{irr} are reported. The magnetization curves are reversible and a linear behaviour is observed at high fields, consistent with the antiferromagnetic character of the particles, in an increasingly extended range with decreasing temperature. Below T_{max}, a hysteretic behaviour is observed, without saturation of the magnetization (Fig. 4). The hysteresis loops are symmetric about the origin. At 5 K the cycles are irreversible for fields up to ∼40 kOe. The temperature dependence of the coercive field is reported in Figure 5. It follows a $(T/T_B)^{1/2}$ dependence, as expected for an assembly of non-interacting single-domain particles with random uniaxial anisotropy, according to the Stoner-Wohlfarth model [21], with $T_B = 17(1)$ K, coherent with T_{max}.

The temperature dependence of the remanent magnetization, M_r, is reported in Figure 6. The data were collected measuring M_r from the hysteresis cycles at different temperatures as well as after cooling the sample from room temperature (RT) down to 5 K in an applied magnetic field of 50 kOe, then switching off the field and measuring the zero field magnetization with increasing temperature.

Hysteresis loops were also measured at the same temperatures below T_{max}, after FC from 150 K in a field of 50 kOe (Fig. 7). The FC loop is shifted along the field axis with respect to the ZFC loop. The exchange field H_E, i.e. the loop displacement, decreases rapidly with temperature, vanishing at about 20 K (Fig. 8).

Discussion

Since the particle dispersion in the polymer is very diluted, inter-particle interactions are expected to be negligible. This allows us to derive the average particle

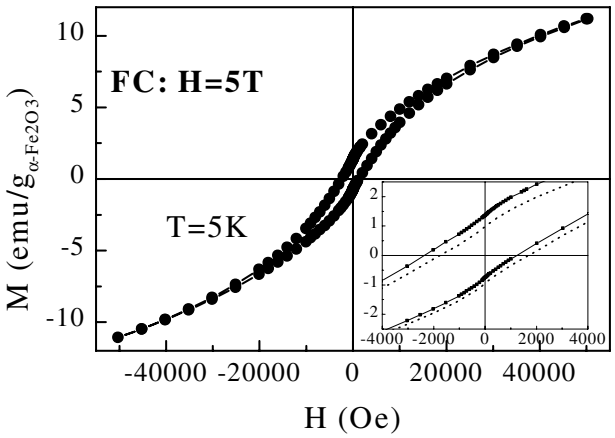

Fig. 7. Hysteresis loops at 5 K after FC in 50 kOe. The inset shows the low field magnetization response; the dotted line corresponds to the ZFC cycle.

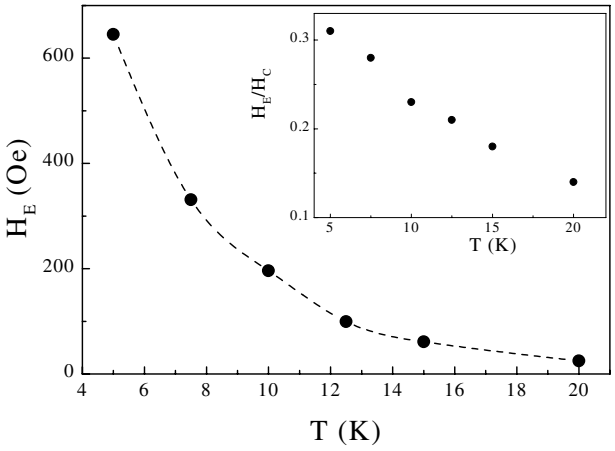

Fig. 8. Exchange field, H_E as a function of temperature. Inset: normalized exchange field, H_E/H_C vs. T.

moment and particle size from magnetization measurements as a function of magnetic field in the superparamagnetic regime. At $T > T_{irr}$, the temperature and field dependence of the magnetization of an assembly of identical, non-interacting, single-domain nanoparticles is described by the Boltzmann' statistics for a random distribution of anisotropy axes directions weighted by the size distribution function (log-normal distribution in our case) [15,22]. A non-linear least-square fit of the magnetization data for the $M(H)$ curves at $T \geq 100$ K was performed using the expression:

$$M(H,T) = \frac{1}{Z}\int_0^\infty dV\, f(V) \int_0^\pi d\alpha \int_0^\pi \sin(\theta)\, d\theta \times \int_0^{2\pi} d\varphi\, \mu(V)\, \cos(\theta)\, \exp\left[\frac{\mu(V)H\cos^2\theta - KV\cos^2\psi(\theta,\varphi,\alpha)}{k_BT}\right] + \chi H \quad (1)$$

with

$$Z = \int_0^\infty dV\, f(V) \int_0^\pi d\alpha \int_0^\pi \sin(\theta)\, d\theta \times \int_0^{2\pi} d\varphi\, \exp\left[\frac{\mu(V)H\cos^2\theta - KV\cos^2\psi(\theta,\varphi,\alpha)}{k_BT}\right],$$

where $f(V)$ is the lognormal volume distribution, θ is the angle between the magnetic moment and the field, φ is the azimutal angle, ψ is the angle between the magnetic moment and the anisotropy axis and α is the angle between the magnetic field and the anisotropy axis.

It was assumed, in a first approximation, a $V^{2/3}$ dependence of μ, being the magnetic moment mainly due to the disordered surface layer [15,23], as the core net moment, produced by the non exact compensation of the two magnetic sublattices, should be small. The linear term χH accounts for the linear variation at high fields (above ≈10 kOe), due to the core antiferromagnetic contribution, responsible for the non-saturation of the magnetization. The fit of the experimental data to equation (1) (solid line in Fig. 3) is satisfactory and the mean magnetic moment of the distribution (extrapolated at $T = 0$) $\langle\mu_0\rangle \approx (76 \pm 15)\mu_B$ (with a $\sigma_\mu = 0.56$) and an average size $\langle\phi_0\rangle = (6 \pm 1)$ nm (to be compared to the value of 5 nm measured by TEM) were derived. Since the dispersion of the hematite nanoparticles in PVA is 3.6% volume fraction, the deduced interparticle distance is $d \sim 3.2\langle\phi\rangle \sim 19$ nm. For such large distances, the dipole-dipole inter-particle interactions are very weak, and can be considered negligible.

For an assembly of non interacting nanoparticles, the energy barrier distribution, $f(E_B)$, may be obtained by differentiation of the remanence vs. temperature curve [24]. This distribution is related to the blocking temperature distribution, $f(T_B)$, taking $E_B = K_aV$. The inset of Figure 6 shows $f(T_B)$, derived from the differentiation of the M_r curve. There is a maximum at 18 K (coherent with T_{max}) according to a lognormal distribution of T_B with $\sigma = 0.57$, corresponding to a value of $\sigma_d = 0.2$ in the lognormal distribution of the diameter.

For non interacting uniaxial single-domain nanoparticles, the relaxation time is described by the Néel-Brown model [25]: $\tau = \tau_0\, \exp(E_B/k_BT)$, where $\tau_0 \sim 10^{-10}$ s for antiferromagnetic particles. For a particle of volume V, when $\tau = t_m$ (measuring time) (≈100 s for DC susceptibility measurements), $T = T_B$. Under these assumptions, taking $T_B = 18$ K and V corresponding to a particle diameter of 5 nm, the deduced anisotropy constant is $K_a \sim 8 \times 10^5$ erg/cm^3. This value, much higher than that for bulk hematite ($K_a = 8\times10^4$ erg/cm^3 [26]), is similar to that obtained on hematite particles of similar size by low temperature magnetization measurements [8]. Moreover, the analysis of the hysteresis loops below T_{irr} (Figs. 4, 5) reveals the existence of a large effective anisotropy, as indicated by a large coercive field ($H_c = 1730$ Oe) and a very large irreversibility field ($H_{irr} \sim 43000$ Oe), below which the decreasing and increasing branches of the magnetization curve separate.

With decreasing temperature, particle moments block progressively and surface spins fluctuations are expected to slow down, until they freeze in random directions at low temperature, giving rise to a disordered magnetic structure, spin-glass or cluster glass like, characterized by multiple spin configurations. This is supported by the observation at low temperature (below 20 K) of shifted hysteresis loops, after field cooling, revealing exchange anisotropy effects, due to the exchange coupling between the different core and surface magnetic structures, antiferromagnetically (uncompensated) ordered and frozen disordered, respectively, as observed in other antiferromagnetic nanoparticle systems [27,28]. Such exchange coupling results in shifted hysteresis loops because field cooling selects a surface spin configuration favouring the particle to be magnetized in the field direction. The values of H_E are plotted in Figure 8, showing that H_E decreases rapidly with increasing temperature, faster than H_C, as can be seen in the inset where H_E/H_C vs. T is plotted.

Conclusions

We have investigated by magnetization measurements the magnetic properties of 5 nm α-Fe_2O_3 nanoparticles dispersed in a polymer. The results indicate that the magnetic behaviour is mainly determined by surface effects, which manifest themselves in high coercive fields, high irreversibility field, and shifted hysteresis loops, after field cooling. These effects come from surface anisotropy and exchange anisotropy, due to the coupling between the disordered surface magnetic structure, with multiple spin configurations, and the core antiferromagnetically ordered structure.

This work has been accomplished with partial support by CONICET-CNR (Argentine-Italy) cooperation project and by PICT 3-6340 (Argentina) project.

References

1. O. Iglesias, A. Labarta, Phys. Rev. B **63**, 184416 (2001)
2. R.H. Kodama, A.E Berkovitz, E.J. Mc Niff, Jr, S. Foner, Phys. Rev. Lett. **77**, 394 (1996)
3. E. Tronc, A. Ezir, R. Cherkaoui, C. Chanéac, M. Nogues, H. Kachkachi, D. Fiorani, A.M. Testa, J.M. Grenèche, J.P. Jolivet, J. Magn. Magn. Mater. **221**, 63 (2000)
4. E. De Biasi, C.A. Ramos, R.D. Zysler, H. Romero, Phys. Rev. B **65**, 144416 (2002)
5. E. De Biasi, R.D. Zysler, C.A. Ramos, H. Romero, Physica B **320**, 203 (2002)
6. R.H. Kodama, J. Magn. Magn. Mater. **200**, 359 (1999)
7. H. Kachkachi, A. Ezzir, M. Noguès, E. Tronc, Eur. Phys. J. B **14**, 681 (2000)
8. E. del Barco, M. Duran, J.M. Hernandez, J. Tejada, R.D. Zysler, M. Vasquez Mansilla, D. Fiorani, Phys. Rev. B **65**, 052404 (2002)
9. R.H. Kodama, S.A. Makholouf, A.E. Berkovitz, Phys. Rev. Lett. **79**, 1393 (1997)
10. D.V. Dimitrov, G.V. Hadjipanayis, V. Papaefthymiou, A.J. Simopoulos, J. Magn. Magn. Mater. **188**, 8 (1998)
11. M. Hansen, F. Bødker, S. Mørup, K. Lefmann, K.N. Clausen, P.A. Lindgard, Phys. Rev. Lett. **79**, 4910 (1997)
12. F. Bødker, M. Hansen, C.N. Koch, K. Lefmann, S. Mørup, Phys. Rev. B **61**, 6826 (2000)
13. R. Zysler, D. Fiorani, J.L. Dormann, A.M. Testa, J. Magn. Magn. Mater. **133**, 71 (1994)
14. L. Suber, D. Fiorani, P. Imperatori, S. Foglia, A. Montone, R. Zysler, Nanostr. Mater. **11**, 797 (1999)
15. M. Vasquez-Mansilla, R.D. Zysler, C. Arciprete, M.I. Dimitrijewits, C. Saragovi, J.M. Greneche, J. Magn. Magn. Mater. **204**, 29 (1999)
16. C.G. Shull, W.A. Strauser, E.O. Wollan, Phys. Rev. B **83**, 333 (1951)
17. C. Guilland, J. Phys. Radium. **12**, 489 (1951)
18. N. Amin, S. Arajs, Phys. Rev. B **35**, 4810 (1987)
19. M.Z. Dang, D.G. Rancourt, J.E. Dutrizac, G. Lamarche, R. Provencher, Hyperfine Interactions **117**, 271 (1998)
20. J.M. Greneche et al. (to be published)
21. E.C. Stoner, E.P. Wohlfarth, Phil. Trans. Roy. Soc. A **240**, 599 (1948)
22. J.L. Dorman, D. Fiorani, E. Tronc, Advances in Chemical Physics **98**, 283 (1997)
23. J.L. Dorman, Rev. Phys. Appl. **16**, 275 (1981)
24. K.O' Grady, R.W. Chantrell, *Studies of Magnetic Properties and their Relevance to Materials Science*, edited by J.L. Dormann, D. Fiorani (Elsevier Sci. Publ., 1992), p. 93
25. L. Néel, J. Phys. Soc. Jpn **17** (Suppl. B1), 676 (1961)
26. A.H. Morrish, *Canted Antiferromagnetism: Hematite* (World Scientific, Singapure, 1994)
27. S.A. Makhlouf, F.T. Parker, F.E. Spada, A.E. Berkowitz, J. Appl. Phys. **81**, 5561 (1987)
28. S.A. Makhlouf, F.T. Parker, A.E. Berkowitz, Phys. Rev. B **55**, R14719 (1997)